Electric transport and magnetic properties in multilayer graphene

Masaaki Nakamura[1] and Lila Hirasawa[2,3]
[1]*Department of Applied Physics, Faculty of Science, Tokyo University of Science, 1-3 Kagurazaka, Shinjuku-ku, Tokyo 162-8601, Japan*
[2]*Institute for Solid State Physics, University of Tokyo, Kashiwanoha, Kashiwa-shi, Chiba 277-8581, Japan*
[3]*Department of Physics, Tokyo Institute of Technology, Oh-Okayama, Meguro-ku, Tokyo 152-8551, Japan*
(Received 31 October 2007; published 29 January 2008)

We discuss electric transport and orbital magnetism of multilayer graphenes in a weak-magnetic field using the matrix decomposition technique. At zero temperature, the minimum conductivity is given by that of the monolayer system multiplied by the layer number N, independent of the interlayer hopping t. When the interlayer hopping satisfies the condition $t \gg \hbar/\tau$ with τ being collision time of impurity scattering, $[N/2]$ kinks and $[N/2]+1$ plateaux appear in the Fermi-energy (gate voltage) dependence of the conductivity and the Hall conductivity, respectively. These behaviors are interpreted as multiband effects. We also found that the Hall conductivity and the magnetic susceptibility take minimum value as a function of temperature, for certain value of the gate voltage. This behavior is explained by Fermi-energy dependence of these functions at zero temperature.

DOI: 10.1103/PhysRevB.77.045429 PACS number(s): 73.43.Cd, 71.70.Di, 81.05.Uw, 72.80.Le

I. INTRODUCTION

Experimental studies of graphene have revealed exotic transport properties, such as an anomalous quantum Hall effect and the finite universal conductivity at zero energy.[1,2] These results are essentially explained by the two-dimensional (2D) massless Dirac equation which describes the low-energy band structure of graphene around the gapless point.[3–9] Moreover, multilayer graphenes which consist of stacked few-layer systems also attract attention. For bilayer systems, quantum Hall effect[1,2,10] and longitudinal conductivity[11–14] have been studied. For systems with more than three layers, electronic structures are investigated experimentally[15–17] and theoretically.[18–20] One of the most interesting points of these multilayer systems would be variety of stacking structures. A graphene is usually produced by micromechanical cleavage of graphite, so that the stacking structure is considered to be the Bernal type, since the natural graphite falls into this category. However, production of graphene with other stacking types may also be possible by recent epitaxial methods. The difference of band structure depending on the stacking types are discussed,[19,20] and stability of the stacking structures is also studied in terms of symmetry arguments.[21]

On the other hand, the magnetic susceptibility of carbon systems has been studied for long times, before the discovery of graphene. It is well known that three-dimensional graphite shows large diamagnetism, and this has been explained theoretically by McClure. He showed that the orbital diamagnetism appears with a delta function peak at the zero energy point based on the 2D massless Dirac equation.[22,23] This argument can be essentially applied to monolayer graphenes,[24] and effects of impurity scattering[25,26] and of an energy gap[27] are discussed. The orbital magnetism in multilayer systems was studied more than two decades ago, motivated by graphite intercalation compounds. Especially, the magnetic susceptibility of bilayer and multilayer systems was discussed by Safran[28] and by Saito and Kamimura,[29] respectively. Quite recently, Koshino and Ando calculated the susceptibility using matrix decomposition technique.[30] They discussed that Hamiltonian of the Bernal stacking systems can be block diagonalized into effective bilayer and monolayer Hamiltonians depending on parity of layer numbers. This is a powerful tool to investigate multilayer systems.

In this paper, we turn our attention to the electric conductivity and Hall conductivity of multilayer graphenes in a weak-magnetic field. We also consider how the differences of stacking structures appear in the physical quantities. We use the matrix decomposition technique used by Koshino and Ando throughout this paper for the calculation of Bernal stacking systems. We also discuss the finite-temperature properties including magnetic susceptibility in these systems.

The rest of paper is organized as follows. In Sec. II, we discuss the Hamiltonian of the multilayer systems. In Secs. III and IV, the conductivity and the Hall conductivity are discussed, respectively. Kinks and plateaux appearing in their Fermi-energy dependence are discussed. In Sec. V, we discuss the finite-temperature properties of the diamagnetic orbital susceptibility, and discuss a minimum value as a function of temperature. In Appendixes, we discuss the decomposition of Hamiltonian, and present analytical forms of physical quantities.

II. STACKING STRUCTURES

As is well known, the band structure of graphene has two gapless points due to the hexagonal lattice, and the low-energy property of this system is described by the 2D massless Dirac equation. For the multilayer graphene, we consider network of the Dirac fermion systems connected by interlayer hopping t. It is also known that there are mainly two stacking types for graphite: one is the Bernal (staggered) stacking where the layer sequence can be written 1212…, and the other is rhombohedral stacking 123123… (see Fig. 1).

The Hamiltonians of the Bernal stacking systems are given by

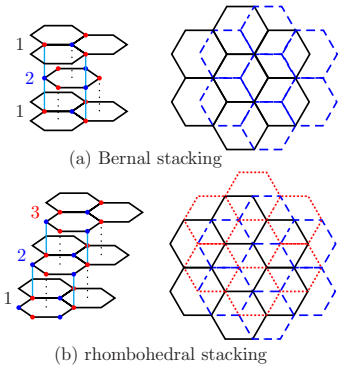

FIG. 1. (Color online) Two stacking structures of multilayer graphene.

$$\mathcal{H}_b = \begin{bmatrix} & \tilde{\pi}_- & t & & & & & & \\ \tilde{\pi}_+ & & & & & & & & \\ & & \tilde{\pi}_- & & & & & & \\ t & & \tilde{\pi}_+ & & t & & & & \\ & & & t & & \tilde{\pi}_- & & t & \\ & & & & \tilde{\pi}_+ & & & & \\ & & & & & & \tilde{\pi}_- & & \\ & & & & t & & \tilde{\pi}_+ & & t \\ & & & & & & & t & \end{bmatrix}, \quad (1)$$

where $\tilde{\pi}_\pm \equiv v\pi_\pm$ with v being the velocity of the Dirac equation for the monolayer system, and $\pi_\pm \equiv \pi_x \pm i\pi_y$. $\boldsymbol{\pi} \equiv \boldsymbol{p} + e\boldsymbol{A}/c$ is the momentum operator in a magnetic field $\nabla \times \boldsymbol{A} = (0,0,B)$. The band structures obtained as eigenvalues of this Hamiltonian are shown in Fig. 2. Quite recently, Koshino and Ando proved that the effective Hamiltonian of N-layer Bernal stacking system becomes, without loss of generality, isolated $[N/2]$ bilayer system ($[x]$ is the maximum integer which does not exceed x) with effective interlayer hoppings $t_1^*, t_2^*, \ldots, t_{[N/2]}^*$, and one monolayer system if N is odd.[30] This result can also be obtained by calculating determinant of the Schrödinger equation (see Appendix A). The values of effective hoppings are given in Table I. We will use this decomposed effective Hamiltonian throughout this paper. For the bilayer system, an energy gap $\Delta = t$ between two bands appears, since the energy spectra are given by $\varepsilon = \pm(\sqrt{t^2 + (2v\hbar k)^2} \pm t)/2$.

TABLE I. Effective interlayer hopping integral t_i^* ($i = 1, 2, \ldots, [N/2]$) of the effective bilayer Hamiltonian of the Bernal stacking systems.

N	t_1^*/t	t_2^*/t	t_3^*/t	$\cdots$
2	1			
3	$\sqrt{2}$			
4	$\frac{\sqrt{5}-1}{2}$	$\frac{\sqrt{5}+1}{2}$		
5	1	$\sqrt{3}$		

On the other hand, the rhombohedral stacking is described by

$$\mathcal{H}_r = \begin{bmatrix} & \tilde{\pi}_- & t & & & & & & \\ \tilde{\pi}_+ & & & & & & & & \\ & & \tilde{\pi}_- & & t & & & & \\ t & & \tilde{\pi}_+ & & & & & & \\ & & & & \tilde{\pi}_- & & t & & \\ & t & & \tilde{\pi}_+ & & & & & \\ & & & & & & \tilde{\pi}_- & & \\ & & & t & & \tilde{\pi}_+ & & & \end{bmatrix}. \quad (2)$$

The band structure of this system is complicated, as shown in Fig. 2, and decomposition such as the Bernal stacking is difficult. If we turn our attention to the two bands near the zero-energy point, the effective Hamiltonian becomes the following 2×2 form[10,21] (see Appendix A)

$$\mathcal{H}_{\text{eff}} = -\frac{1}{t^{N-1}} \begin{bmatrix} 0 & (v\pi_+)^N \\ (v\pi_-)^N & 0 \end{bmatrix}. \quad (3)$$

This effective Hamiltonian is useful to discuss the quantum Hall effect[10] and the zero-energy longitudinal conduc-

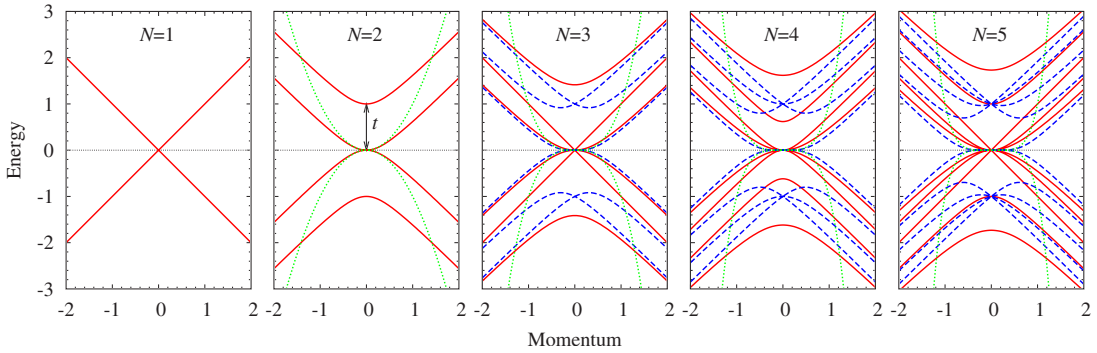

FIG. 2. (Color online) Band structure of multilayer systems ($N = 1-5$) with the Bernal stacking [Eq. (1), solid line] and with the rhombohedral stacking [Eq. (2), dashed line]. For the Bernal stacking, linear dispersion relations appear for odd layer cases. The dispersion relation of the effective Hamiltonian of the rhombohedral stacking [Eq. (3), dotted line] is also shown.

tivity,[13,14] but it is difficult to obtain physically relevant results for the Hall conductivity and the susceptibility in the weak-magnetic field treatment below (see Appendix B). Therefore, calculations in this paper is mainly devoted to Bernal stacking systems.

The low-energy effective Hamiltonian (3), however, gives information of the reason why the Bernal stacking is more stable than the rhombohedral stacking: Since the dispersion relation is $\varepsilon = \pm (v\hbar k)^N / t^{N-1}$, the density of states of the N-layer rhombohedral system is given by

$$D_N(\varepsilon) = \frac{Vt}{2\pi N \hbar^2 v^2} \left(\frac{|\varepsilon|}{t} \right)^{2/N-1}, \tag{4}$$

where V is volume of the system. For $N \geq 3$, $D_N(\varepsilon)$ diverges at $\varepsilon = 0$, where the density of states of the Bernal case is const. Therefore, the rhombohedral systems are considered to be unstable against external perturbations.

III. CONDUCTIVITY

First, we consider the conductivity of the multilayer systems based on the linear response theory. The conductivity is given by the Kubo formula[31]

$$\mathrm{Re}\ \sigma_{\mu\nu} = \lim_{\omega \to 0} \frac{\mathrm{Im}\ \tilde{\Pi}_{\mu\nu}(\mathbf{0}, \omega + i0)}{\hbar \omega}, \tag{5}$$

where $\tilde{\Pi}_{\mu\nu}(\boldsymbol{q}, \omega) \equiv \Pi_{\mu\nu}(\boldsymbol{q}, \omega) - \Pi_{\mu\nu}(\boldsymbol{q}, 0)$. The polarization function in the Matsubara form is given by

$$\Pi_{\mu\nu}(\boldsymbol{q}, i\nu_m) = \frac{1}{V} \int_0^{\beta\hbar} d\tau e^{i\nu_m \tau} \langle \mathcal{T}_\tau J_\mu(\boldsymbol{q}, \tau) J_\nu(\mathbf{0}, 0) \rangle, \tag{6}$$

$$\tilde{\Pi}_{\mu\nu}(\mathbf{0}, i\nu_m) = -\frac{e^2}{\beta\hbar V} \sum_{\boldsymbol{k}} \sum_n \mathrm{tr}(\mathcal{G} \gamma_\mu \mathcal{G}_+ \gamma_\nu), \tag{7}$$

where $\beta \equiv 1/k_B T$ and V are the inverse temperature and the volume of the system, respectively. The current operator is given by

$$J_\mu(-\boldsymbol{q}, \tau) = -e \sum_{\boldsymbol{k}} \Psi^\dagger(\boldsymbol{k} + \boldsymbol{q}/2, \tau) \gamma_\mu \Psi(\boldsymbol{k} - \boldsymbol{q}/2, \tau), \tag{8}$$

where $\Psi(\boldsymbol{k}, \tau)$ is the Fourier component of the field operator $\Psi^\dagger(\boldsymbol{r}) = [\psi^\dagger_{A_1}(\boldsymbol{r}), \psi^\dagger_{B_1}(\boldsymbol{r}), \psi^\dagger_{A_2}(\boldsymbol{r}), \psi^\dagger_{B_2}(\boldsymbol{r}), \ldots]$, where A_i and B_i indicate two sublattices of the hexagonal lattice of ith layer. The matrix γ_μ is defined by

$$\gamma_\mu \equiv \frac{1}{\hbar} \frac{\partial \mathcal{H}}{\partial k_\mu}. \tag{9}$$

In Eq. (7), the impurity-averaged temperature Green function is given by

$$\mathcal{G} \equiv \mathcal{G}(\boldsymbol{k}, i\omega_n) = (i\omega_n + [\mu + i\, \mathrm{sgn}(\omega_n)\Gamma - \mathcal{H}_0]/\hbar)^{-1}, \tag{10}$$

where $\omega_n \equiv (2n+1)\pi/\beta\hbar$ is the Matsubara frequency of fermions. For $\mathcal{G}_+ \equiv \mathcal{G}(\boldsymbol{k}, \omega_n + \nu_m)$, $\nu_m = 2\pi m/\beta\hbar$ is the Matsubara frequency of bosons. Here, we have introduced the scattering rate phenomenologically as the quasiparticle self-energy $\Gamma = -\mathrm{Im}\ \Sigma^R$, neglecting the frequency and the momentum dependences. This parameter stems from the scattering of the impurity potential implicitly assumed in the present system, and is related to the mean free time of quasiparticles as $\Gamma = \hbar/2\tau$.[32]

The final analytic form of σ_{xx} for a bilayer system is presented in Appendix B. In Fig. 3, the zero-temperature conductivity (calculated per valley and per spin) σ_{xx} versus the Fermi energy μ scaled by the scattering rate Γ is shown. Experimentally, μ is a tunable parameter by the gate voltage. At zero energy $\mu/\Gamma = 0$, the conductivity takes the minimum value $\sigma_{xx} = Ne^2/\pi h$ which is the N times of the minimum conductivity of the monolayer system.[3,4,6,7] For this finite value $\sigma_{\min} = e^2/\pi h$, there are controversial arguments,[9] but all the analytic results do not coincide with the experimental value e^2/h,[1,2] except for the numerical analysis of Nomura and MacDonald.[33]

As the Fermi energy increases as $\mu/\Gamma \to \infty$ with small interlayer hopping $t/\Gamma \ll 1$, the conductivity approaches to N times of the Drude-Zener form,

$$\sigma_{xx} = \frac{\sigma_0}{1 + (\omega_c \tau)^2} \simeq \sigma_0 = \frac{e^2 \tau \mu}{4\pi\hbar^2}. \tag{11}$$

Compared with the result of the linearized Boltzmann equation for nonrelativistic electrons $\sigma_0 = ne^2\tau/m$, where n is the electron density, the "electron mass" m is related as $m = |\mu|/v^2$.[7] This agreement with the Boltzmann description is due to the constant Γ. A similar linear Fermi-energy dependence of the conductivity is reproduced by numerical calculation considering effects of screened Coulomb impurity scattering.[33]

For large interlayer hopping $t/\Gamma \gg 1$ which means that the energy gap $\Delta \sim O(t)$ satisfies the condition $\Delta \gg \hbar/\tau$, kinks appear in the Fermi-energy dependence. The number of kinks is increased as the layers are increased. These phenomena can be interpreted as a multiband effect: When the interlayer hopping is large enough in the N-layer system, N bands in the positive (negative) energy region split into $[(N+1)/2]$ gapless modes and other bands with different energy gaps. Therefore, the number of kinks in the positive or negative energy region is $N/2$ for even layers, and $(N-1)/2$ for odd layers, reflecting the discontinuity of the density of states.

In order to clarify this argument, we generalize Eq. (11) to the multiband system for $\mu \geq 0$ as

$$\sigma_{xx} = \frac{e^2 \tau}{4\pi\hbar} \sum_{i=1}^{N} \theta(\mu - v_i k_{F,i}) v_i k_{F,i}, \tag{12}$$

where the velocity v_i and the Fermi wave number of the ith band $k_{F,i}$ are related as

$$m v_i = \hbar k_{F,i}, \quad \mu = \varepsilon_i(k_{F,i}). \tag{13}$$

In Fig. 4, the Fermi-energy dependence of the zero-temperature conductivity at $t/\Gamma = 6$ for various layer numbers

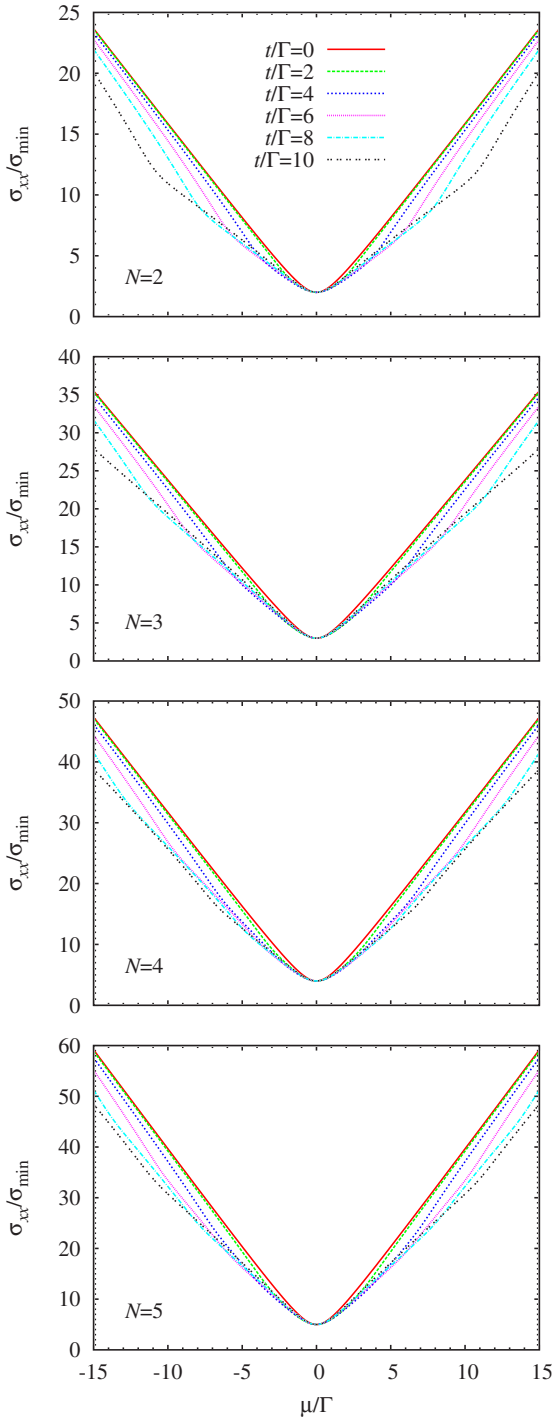

FIG. 3. (Color online) Fermi-energy (μ/Γ) dependence of the longitudinal conductivity of Bernal stacking systems with $N=2,3,4,5$, scaled by the minimum conductivity of the monolayer system $\sigma_{\min}=e^2/\pi h$. In these results, $[N/2]$ kinks appear for the positive (or negative) Fermi-energy regions.

is shown. The results of semiclassical analysis show good agreement with those of the linear response theory, except for the small energy region where the quantum effect is essential. For more detailed semiclassical argument, we should consider the Boltzmann equation for Dirac type systems.[34]

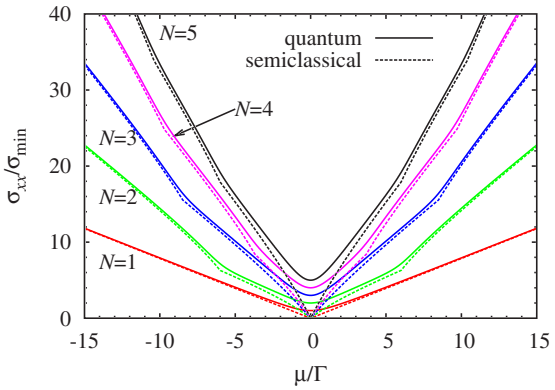

FIG. 4. (Color online) Comparison between the longitudinal conductivity obtained by the linear response theory (solid lines) and that by the semiclassical analysis (dashed lines) for one to five layer systems with $t/\Gamma=6$.

IV. HALL EFFECT

Next, we consider the Hall conductivity σ_{xy} in a weak-magnetic field. The expression of the Hall conductivity in terms of the Green function is obtained by the Luttinger-Kohn representation[35] for the basic functions and the Fourier expansion of the vector potential $\boldsymbol{A}(\boldsymbol{r})=\boldsymbol{A}_{\boldsymbol{q}}e^{i\boldsymbol{q}\cdot\boldsymbol{r}}$. As the first-order perturbation of the current term of the Hamiltonian $\mathcal{H}-\boldsymbol{A}_{\boldsymbol{q}}\cdot\boldsymbol{J}(-\boldsymbol{q})/c$, we have the following three point function:[36–38]

$$\Pi_{\mu\nu}(\boldsymbol{q},i\nu_m)=\sum_{\alpha=x,y}\frac{A_{\boldsymbol{q}\alpha}}{c\hbar}\frac{1}{V}\int_0^{\beta\hbar}d\tau\int_0^{\beta\hbar}d\tau' \times e^{i\nu_m\tau}\langle\mathcal{T}_\tau J_\mu(\boldsymbol{q},\tau)J_\alpha(-\boldsymbol{q},\tau')J_\nu(\boldsymbol{0},0)\rangle. \quad (14)$$

Then by $\boldsymbol{q}$ expansion of the temperature Green function with the relation $\partial_{k_\mu}\mathcal{G}=\mathcal{G}\gamma_\mu\mathcal{G}$, we obtain the polarization function in the linear order of the magnetic field $B=i(q_xA^y_{\boldsymbol{q}}-q_yA^x_{\boldsymbol{q}})$ as

$$\tilde{\Pi}_{\mu\nu}(\boldsymbol{0},i\nu_m)=i\frac{e^3B}{2c\hbar}\frac{1}{V\beta\hbar}\sum_{\boldsymbol{k},n}\mathrm{tr}(\gamma_\mu\mathcal{G}_+\gamma_x\mathcal{G}_+\gamma_\nu\mathcal{G}\gamma_y\mathcal{G} - \gamma_\mu\mathcal{G}_+\gamma_y\mathcal{G}_+\gamma_\nu\mathcal{G}\gamma_x\mathcal{G}+\gamma_\mu\mathcal{G}_+\gamma_x\mathcal{G}_+\gamma_y\mathcal{G}_+\gamma_\nu\mathcal{G} - \gamma_\mu\mathcal{G}_+\gamma_y\mathcal{G}_+\gamma_x\mathcal{G}_+\gamma_\nu\mathcal{G}+\gamma_\mu\mathcal{G}_+\gamma_\nu\mathcal{G}\gamma_x\mathcal{G}\gamma_y\mathcal{G} - \gamma_\mu\mathcal{G}_+\gamma_\nu\mathcal{G}\gamma_y\mathcal{G}\gamma_x\mathcal{G}). \quad (15)$$

In Fig. 5, we show the zero-temperature Hall conductivity (calculated per valley and per spin) σ_{xy} versus the Fermi energy (gate voltage) μ scaled by the scattering rate Γ. The Hall conductivity changes the sign depending on the sign of μ. For small t/Γ, the Hall conductivity shows sharp change in the small energy region $\mu/\Gamma\to0$. Then its absolute value takes maximum, and approaches to the constant value ($\propto\Gamma^{-2}$), as the Fermi energy is increased as $\mu/\Gamma\to\infty$. This value is N times of the Drude-Zener-like formula,

$$\sigma_{xy}=\frac{-\omega_c\tau\sigma_0}{1+(\omega_c\tau)^2}\simeq-\omega_c\tau\sigma_0, \quad (16)$$

where $\omega_c=|eB|/mc$ is the cyclotron frequency. The deviation of the Hall conductivity from this classical value at the low-

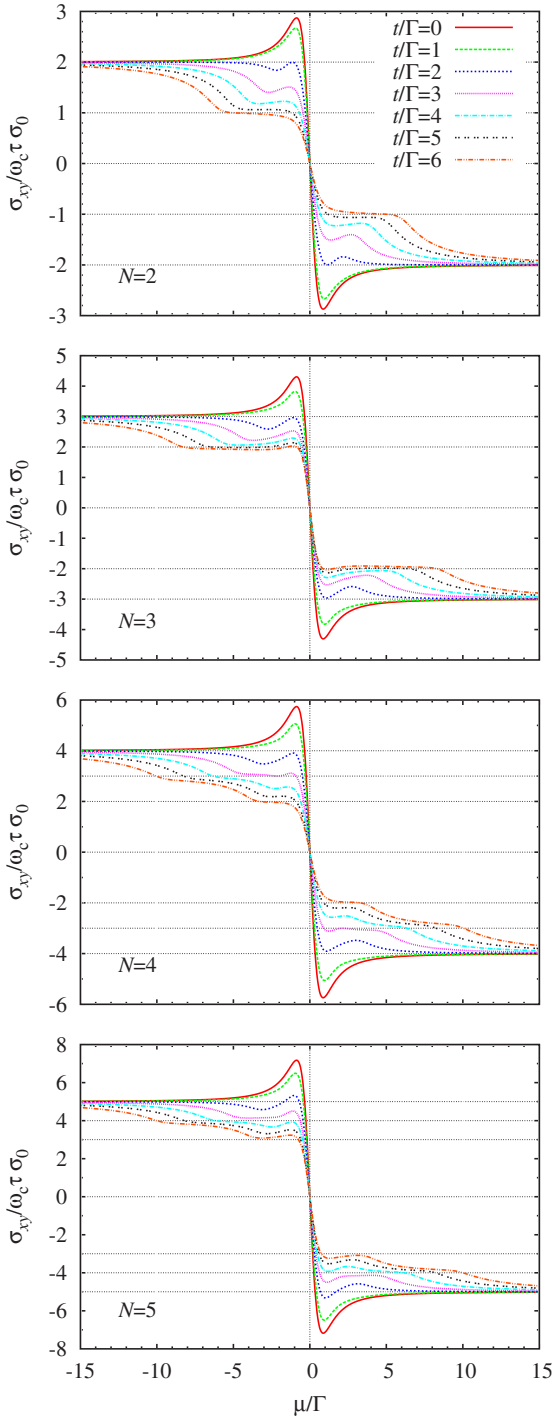

FIG. 5. (Color online) Fermi-energy (μ/Γ) dependence of the Hall conductivity of Bernal stacking systems with $N=2,3,4,5$, scaled by the classical Hall conductivity of the monolayer system $\omega_c\tau\sigma_0$. In these results, $[N/2]+1$ plateaux appear in large t/Γ cases.

energy regions and change of the sign are often called "anomalous" Hall effect. Actually, this behavior is observed experimentally in the gate voltage dependence of hall coefficient $\rho_{xy}=-\sigma_{xy}/[(\sigma_{xx})^2+(\sigma_{xy})^2]$ at the surface of a graphite.[39]

The most remarkable feature of the Hall conductivity is that plateaux appear when the interlayer hopping is large

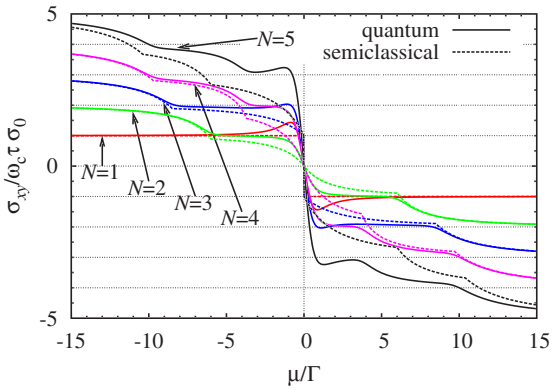

FIG. 6. (Color online) Comparison between the Hall conductivity obtained by the linear response theory (solid lines) and that by the semiclassical analysis (dashed lines) for one to five layer systems with $t/\Gamma=6$.

$t/\Gamma \gg 1$. The number of plateaux for the positive or negative energy regions is $(N+2)/2$ for even layers, and $(N+1)/2$ for odd layers, and σ_{xy} is "quantized" by the unit of $\omega_c\tau\sigma_0$. This phenomenon is due to the effect of the energy gap $\Delta \sim O(t)$ satisfying the condition $\Delta \gg \hbar/\tau$. Actually, a plateau also appears in the result of the monolayer system with an energy gap.[27] In order to clarify this behavior, we also generalize the Drude-Zener theory for σ_{xy} in the multiband systems. Then the Hall conductivity for $\mu \geqslant 0$ is given by

$$\sigma_{xy} = -\omega_c\tau\sigma_{xx} \simeq -\frac{e^3\tau^2 B}{4\pi c\hbar^2}\sum_{i=1}^{N}\theta(\mu - v_i k_{F,i})v_i^2, \qquad (17)$$

where the velocity v_i and "electron mass" m are given by Eq. (13). In Fig. 6, the Fermi-energy dependence of the zero-temperature Hall conductivity σ_{xy} at $t/\Gamma=6$ for various layer numbers is shown. The result of the semiclassical analysis shows good agreement with those of the linear response theory in terms of the step structure of σ_{xy}. For odd layers, the peak structure remains even when the plateaux appear, because of the contribution from a gapless monolayer mode.

We also show in Fig. 7, the Hall conductivity for $N=3$

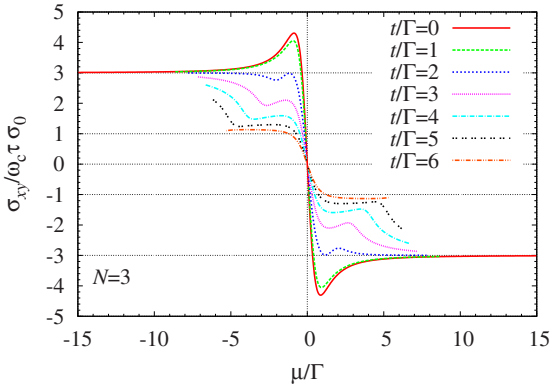

FIG. 7. (Color online) Fermi-energy (μ/Γ) dependence of the Hall conductivity of a rhombohedral stacking system with $N=3$. In this case, the first plateau appears at $\sigma_{xy} \simeq \pm\omega_c\tau\sigma_0$, reflecting the band structure.

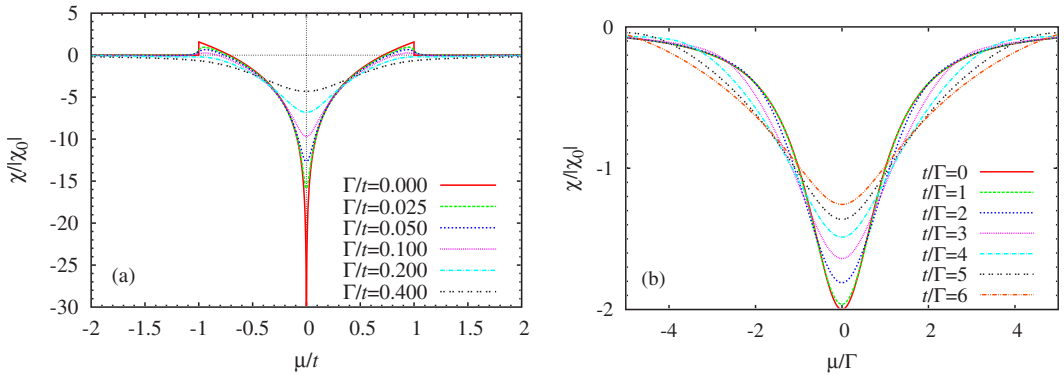

FIG. 8. (Color online) Magnetic susceptibility of the bilayer system at zero temperature as a function of the Fermi energy μ for (a) fixed interlayer hopping $t=1$ and for (b) fixed scattering rate $\Gamma=1$. These data are scaled by $\chi_0=-6e^2v^2/\pi^2c^2$. t dependence of the susceptibility is similar to that of gap dependence in the monolayer system [see Fig. 1(a) of Ref. 27].

rhombohedral stacking system calculated based on the Hamiltonian (2). Reflecting the difference of the band structure (see Fig. 2), the first plateau appears at $\sigma_{xy} \simeq \pm \omega_c \tau \sigma_0$, while $\sigma_{xy} \simeq \pm 2\omega_c \tau \sigma_0$ for Bernal stacking.

V. ORBITAL MAGNETISM AND FINITE-TEMPERATURE PROPERTIES

The orbital magnetism of multilayer graphene with Bernal stacking at zero temperature has already been discussed by Koshino and Ando.[30] Here, we turn our attention to the finite-temperature properties of the magnetic susceptibility. The general formula for the orbital magnetic susceptibility of Bloch electrons was derived by Fukuyama.[40] A modified expression of this formula which is also applicable for the effective Hamiltonian of Eq. (3) (see Appendix B) is

$$\chi = -\frac{2}{\beta V}\left(\frac{e}{c\hbar}\right)^2 \sum_n \sum_{\boldsymbol{k}} \mathrm{tr}(\mathcal{G}\gamma_+\mathcal{G}\gamma_-\mathcal{G}\gamma_+\mathcal{G}\gamma_-), \tag{18}$$

where $\gamma_\pm \equiv (\gamma_x \mp i\gamma_y)/2$. This result is obtained by the Luttinger-Kohn base, the Fourier expansion $\boldsymbol{A}(\boldsymbol{r}) = \boldsymbol{A}_{\boldsymbol{q}}(e^{i\boldsymbol{q}\cdot\boldsymbol{r}} - e^{-i\boldsymbol{q}\cdot\boldsymbol{r}})/2i$, the $\boldsymbol{q}$ expansion of the temperature Green function, and the second derivative of the thermodynamic potential $\chi = -\frac{1}{V}\frac{\partial^2\Omega}{\partial B^2}|_{B=0}$. Here, the magnetic field is given as $B = q_x A^y_{\boldsymbol{q}} - q_y A^x_{\boldsymbol{q}} = (i/2)(q_+ A^-_{\boldsymbol{q}} - q_- A^+_{\boldsymbol{q}})$ with $\boldsymbol{q} \to \boldsymbol{0}$, where $A^\pm_{\boldsymbol{q}} \equiv A^x_{\boldsymbol{q}} \pm iA^y_{\boldsymbol{q}}$.

Figure 8 shows the susceptibility of the bilayer system at zero temperature (see Appendix B). As discussed by Safran,[28] the susceptibility diverges logarithmically at zero-energy point with $\Gamma=0$, and paramagnetic regions appear. As t/Γ is increased, the Lorentzian-like curve becomes broad, and the diamagnetism becomes smaller (larger) at small (large) Fermi-energy region. This behavior is similar to that of the monolayer system with an energy gap.[27] Therefore, as discussed by Koshino and Ando, odd layer systems with Bernal stacking tend to show large diamagnetism than the even layer systems due to the contribution from gapless mode of the effective monolayer.

In Fig. 9, we show the temperature dependence of the susceptibility of monolayer and bilayer systems. We find that there appears the minimum value at finite temperature when the gate voltage satisfies the relation with some critical value $|\mu| > \mu_c$. This phenomenon is explained in the following way: For simplicity, let us consider the susceptibility in the monolayer system with finite Γ,[25]

$$\chi = -\frac{e^2v^2}{6\pi^2c^2}\int_{-\infty}^{\infty} dx f(x)\mathrm{Im}\,\frac{1}{(x+i\Gamma)^2}, \tag{19}$$

where $f(x) \equiv (e^{\beta(x-\mu)}+1)^{-1}$ is the Fermi distribution function. At zero and high temperature limits, Eq. (19) becomes $\chi = -\frac{e^2v^2}{6\pi^2c^2}\frac{\Gamma}{\mu^2+\Gamma^2}$ and $\chi=0$, respectively. In the finite-temperature

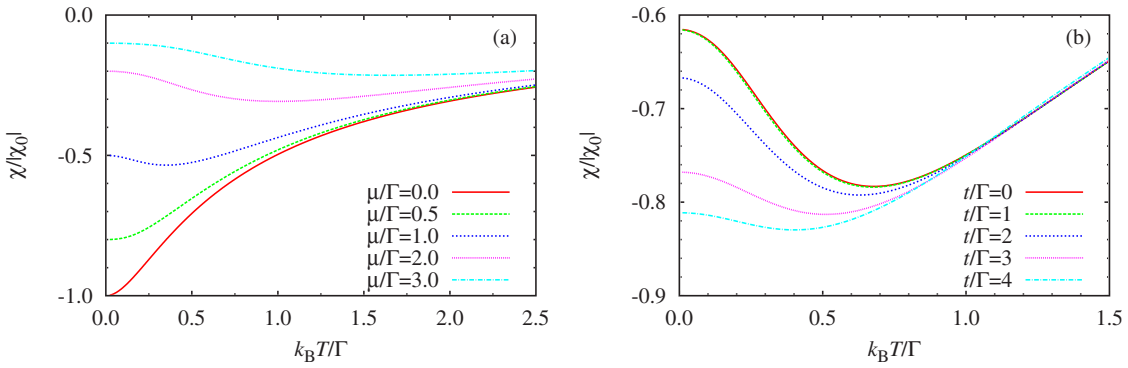

FIG. 9. (Color online) Temperature dependence of the magnetic susceptibility χ of (a) the monolayer system and (b) the bilayer system for several strengths of the interlayer hopping at $\mu/\Gamma=1.5$. A minimum value appears as a function of temperature.

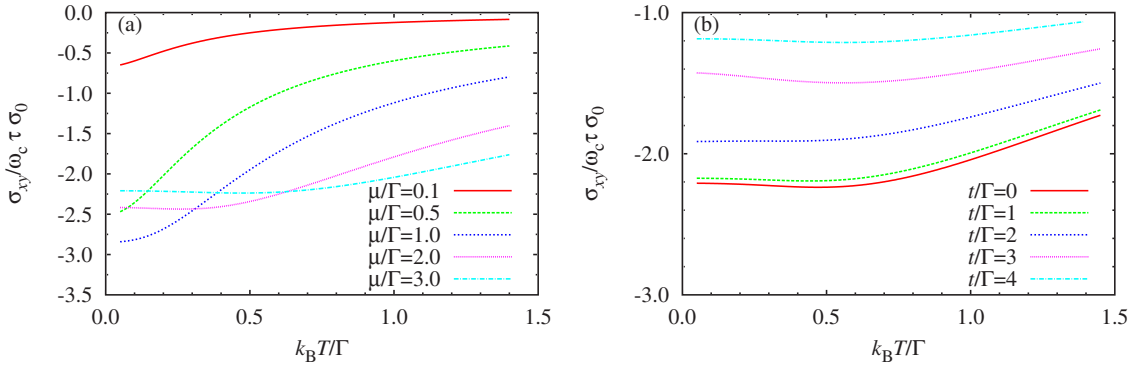

FIG. 10. (Color online) Temperature dependence of the Hall conductivity σ_{xy} of (a) the monolayer system and (b) the bilayer system for several strengths of the interlayer hopping at $\mu/\Gamma=3$. A minimum value appears as a function of temperature.

regions, Sommerfeld expansion of Eq. (19) is

$$\frac{6\pi^2c^2}{e^2v^2}\chi = -\frac{\Gamma}{\mu^2+\Gamma^2} + \frac{\pi^2}{6}(k_BT)^2F'(\mu) + O(k_BT)^3, \quad (20)$$

where

$$F(x) \equiv \mathrm{Im}\,\frac{1}{(x+i\Gamma)^2}, \quad F'(x) = \frac{-2\Gamma[3x^2-\Gamma^2]}{[x^2+\Gamma^2]^3}. \quad (21)$$

Therefore, for $F'(\mu)<0$ ($|\mu|/\Gamma>1/\sqrt{3}$), a minimum value appears as a function of temperature. This means that the condition to appear a minimum value is existence of an inflexion point in the susceptibility at zero temperature as a function of the Fermi-energy $\propto\int_{-\infty}^{\mu}F(x)dx$. The same argument can also be applied to multilayer systems and other physical quantities, and it turns out that the Hall conductivity may have minimum value for small interlayer hopping or odd layer cases (see Fig. 10), where the peak structure of the Hall conductivity is clear. Similar argument for a minimum value of physical quantity at finite temperature is recently done for the magnetization of quantum spin chains in a magnetic field.[41] For the longitudinal conductivity, there appears no minimum (see Fig. 11).

VI. SUMMARY AND DISCUSSION

In summary, we have studied the electric transport and the orbital magnetism of multilayer graphene in a weak-magnetic field. We have found that kinks appear in the gate voltage dependence of the conductivity, and plateaux in the Hall conductivity. These phenomena are explained as multiband effects which become clear when the energy gap and the collision time satisfy the condition $\Delta \gg \hbar/\tau$. We have also considered finite-temperature properties of this system, and found that a minimum value appears in the magnetic susceptibility and the Hall conductivity, as functions of temperature. These phenomena are explained by the existence of an inflexion point in the zero-temperature Fermi-energy dependence.

In this paper, we have turned our attention mainly to the Bernal stacking systems, except for the result of Fig. 7. For rhombohedral stacking systems, the band structure is quite different from that of the Bernal stacking, especially the gapless linear dispersions for odd $N \geqslant 3$ do not appear. Therefore, it is expected that difference of the properties of the physical quantities, such as the magnetic susceptibility, is not so drastic depending on the parity of the number of layers. It is also reported that the trigonal wrapping effect causes essential difference in the longitudinal conductivity.[14] This would be also an interesting future problem. We have also discussed the semiclassical analysis of transport properties using the results of the Boltzmann equation for nonrelativistic electrons. It is expected, however, that the Boltzmann equation for Dirac type systems is needed for more detailed description in regions close to the zero-energy point. Moreover, it is also desirable to extend the present analysis to

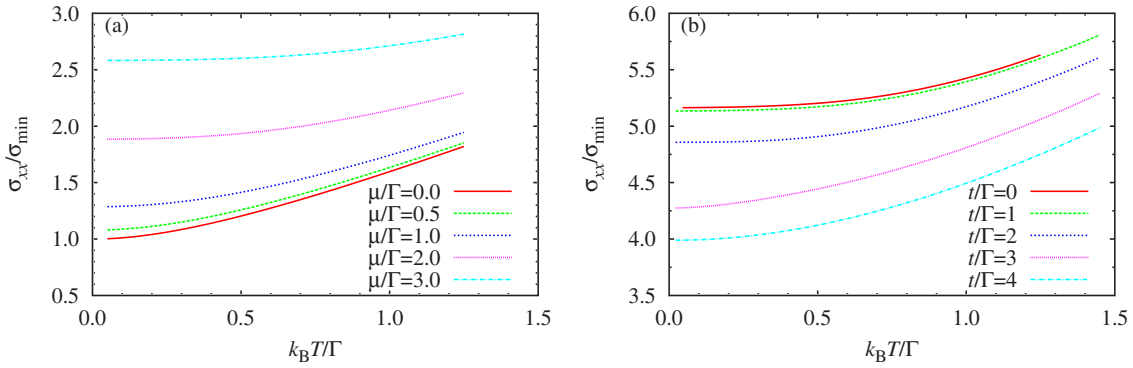

FIG. 11. (Color online) Temperature dependence of the conductivity σ_{xx} of (a) the monolayer system and (b) the bilayer system for several strengths of the interlayer hopping at $\mu/\Gamma=3$. They behave monotonically as a function of temperature.

finite-magnetic field regions where the Landau quantization is essential.

Note added in proof: After the submission of this paper, we became aware of a preprint (H. Min and A. H. MacDonald, arXiv:0711.4333) where the present matrix decomposition technique and the 2×2 effective Hamiltonian are used to discuss the quantum Hall effect in multilayer graphenes with general stacking structures.

ACKNOWLEDGMENTS

The authors are grateful to M. Oshikawa and A. Tokuno for discussions. M.N. thanks T. Ando and A. H. MacDonald for valuable comments.

APPENDIX A: DERIVATION OF THE EFFECTIVE HAMILTONIAN

In order to calculate physical quantities of multilayer systems, it is useful to reduce the original Hamiltonian with $2N\times2N$ matrix form into some effective Hamiltonian which has fewer matrix elements. McCann and Fal'ko reduced the 4×4 matrix Hamiltonian into the 2×2 form to discuss the quantum Hall effect of the bilayer system, which describes the two bands near the zero-energy point.[10] In order to derive such effective Hamiltonian, we should find $\mathcal{H}_{\text{eff}}$ which have the same eigenvalues of the original Hamiltonian $\mathcal{H}$:

$$\det(\varepsilon-\mathcal{H})=\det(\varepsilon-\mathcal{H}_{\text{eff}})=0. \tag{A1}$$

For the rhombohedral N-layer system (2), the 2×2 effective Hamiltonian is obtained in the following way: First, we change the order of the matrix elements from $A_1,B_1,A_2,B_2,\cdots$ to $\cdots B_3,A_2,B_1,A_1,B_2,A_3,\ldots$, where A_i and B_i indicate two sublattices of the hexagonal lattice of ith layer. Then, we have

$$\mathcal{H}=\begin{bmatrix}
\ddots & t & & & & & & \\
t & & & & & & k_- & \\
 & & t & & & k_+ & & \\
 & t & & & k_- & & & \\
 & & & k_+ & & & & \\
 & & k_- & & t & & & \\
 & k_+ & & t & & & & \\
k_- & & & & & & t & \\
 & & & & & t & & \ddots
\end{bmatrix}, \tag{A2}$$

where $k_\pm\equiv k_x\pm ik_y$ is eigenvalue of the momentum operator π_+. We have set $v=\hbar=1$ for simplicity. Next, we calculate $\det(\varepsilon-\mathcal{H})$ approximately for $\varepsilon\ll t$, then we obtain

$$\det(\varepsilon-\mathcal{H})\simeq\varepsilon^2t^{2N-2}-k^{2N}=0. \tag{A3}$$

One of effective Hamiltonians which satisfies Eqs. (A1) and (A3) can be chosen as Eq. (3).

On the other hand, the effective Hamiltonian for the Bernal stacking graphenes is discussed by Koshino and Ando, quite recently.[30] According to their result, N-layer Bernal stacking system can be described by isolated $[N/2]$ bilayer systems with some effective interlayer hopping, and one monolayer system if N is odd. This is exact mapping of Eq. (1) without using any approximation. Here, we derive the same result by the argument based on the determinants. After the same reordering of the original Hamiltonian (1) as the rhombohedral stacking, we have

$$\mathcal{H}=\begin{bmatrix}
\ddots & & & & & & \cdot \\
 & & & & & k_+ & \\
 & & & & k_- & & \\
 & & & k_+ & & & \\
 & & k_- & & t & & \\
 & k_+ & & t & & t & \\
k_- & & & & t & & t \\
\cdot & & & & & t & \ddots
\end{bmatrix}. \tag{A4}$$

Then, we obtain the following recursion relation for the determinant of the N-layer system $A_N\equiv\det(\varepsilon-\mathcal{H})$ as

$$A_1=\varepsilon^2-k^2, \tag{A5}$$

$$A_2=(\varepsilon^2-k^2)^2-t^2\varepsilon^2, \tag{A6}$$

$$\cdots$$

$$A_N=(\varepsilon^2-k^2)A_{N-1}-t^2\varepsilon^2A_{N-2}. \tag{A7}$$

Note that recursion relation such a closed form cannot be obtained for the rhombohedral stacking. Equation (A7) can be solved exactly, and factorized in the following way:

$$A_1\equiv X,$$

$$A_2=X^2-t^2\varepsilon^2,$$

$$A_3=X(X^2-2t^2\varepsilon^2),$$

$$A_4=\left[X^2-\left(\frac{\sqrt{5}-1}{2}\right)^2t^2\varepsilon^2\right]\left[X^2-\left(\frac{\sqrt{5}+1}{2}\right)^2t^2\varepsilon^2\right],$$

$$A_5=X(X^2-t^2\varepsilon^2)(X^2-3t^2\varepsilon^2),$$

$$\cdots.$$

Thus, the determinant for the N-layer system can be decomposed into those of the bilayers $[X^2-(t^*)^2\varepsilon^2]$ with the effective hopping t^* (Table I) and that of one monolayer X for odd N. This means that the original Hamiltonian (1) can be block diagonalized into subsystems. Koshino and Ando have obtained the effective hopping as $t^*=2t\sin[m\pi/2(N+1)]$ with m being an appropriate integer, by considering diagonalization of the matrix (A4).[30] This factorization of the Hamiltonian is analogous to the N-leg ladder in quantum spin systems where a flat dispersion appears for odd N.[42]

APPENDIX B: ANALYTIC RESULTS

Here, we present anaclitic forms of physical quantities discussed in this paper. We also briefly discuss the results based on the low-energy effective Hamiltonian of the rhombohedral stacking (3) given by 2×2 matrix.

The longitudinal conductivity is given by the following form:

$$\sigma = \frac{e^2}{4\pi^2\hbar}\int_{-\infty}^{\infty} dx[-f'(x)]\mathcal{A}_N(x), \tag{B1}$$

where $f(x)=(e^{\beta(x-\mu)}+1)^{-1}$. For the monolayer case $N=1$, we have

$$\mathcal{A}_1(x) = \frac{\Gamma^2+x^2}{\Gamma x}\tan^{-1}\left(\frac{x}{\Gamma}\right)+1. \tag{B2}$$

For the bilayer system $N=2$ with 4×4 Hamiltonian, the result is

$$\begin{aligned}\mathcal{A}_2(x) = &-\frac{tx^2}{\Gamma(t^2-4x^2)}\left\{\frac{\pi}{2}-\tan^{-1}\left(\frac{-t^2+\Gamma^2+x^2}{2t\Gamma}\right)\right\}\\ &+\frac{t\Gamma^2}{(t^2+4\Gamma^2)x}\tanh^{-1}\left(\frac{2tx}{t^2+\Gamma^2+x^2}\right)\\ &+\frac{x^2+\Gamma^2}{2\Gamma x}\left(\frac{t^4}{(t^2-4x^2)(t^2+4\Gamma^2)}+1\right)\left\{2\tan^{-1}\left(\frac{x}{\Gamma}\right)\right.\\ &\left.-\tan^{-1}\left(\frac{t^2+\Gamma^2-x^2}{2x\Gamma}\right)+\frac{\pi}{2}\,\mathrm{sgn}(x)\right\}+2.\end{aligned} \tag{B3}$$

For the 2×2 Hamiltonian (3), σ_{xx} is given by N times of Eq. (B1) with Eq. (B2). This is consistent with the result of Ref. 13 where $N=2$ and $\Gamma=\mu=0$ case is discussed.

We omit the analytical result of the Hall conductivity σ_{xy} for the bilayer system, because of its lengthiness. For σ_{xy} of the 2×2 Hamiltonian (3), the following two terms should be added in tr $(\cdots)$ of the polarization function (15), since γ_μ has momentum dependence,

$$-\mathcal{G}\gamma_x\mathcal{G}_+\gamma_y\mathcal{G}_+(\partial_{k_x}\gamma_y)+\mathcal{G}\gamma_x\mathcal{G}_+(\partial_{k_x}\gamma_y)\mathcal{G}\gamma_y. \tag{B4}$$

In this case, finite cutoff is needed to make the σ_{xy} finite. Moreover, the Drude-Zener-like behavior for the high-energy region cannot be described. As a result, it turns out that Hamiltonian (3) is not appropriate to discuss the Hall conductivity in a weak-magnetic field.

The magnetic susceptibility (18) for bilayer system with 4×4 Hamiltonian is obtained as

$$\chi = \frac{v^2e^2}{12\pi^2c^2}\int_{-\infty}^{\infty} dx f(x)\mathcal{B}_2(x), \tag{B5}$$

and

$$\mathcal{B}_2(x) = \mathrm{Im}\left[\frac{2}{(x+i\Gamma)^2-t^2}-\frac{3}{t(x+i\Gamma)}\log\left[\frac{t+x+i\Gamma}{-t+x+i\Gamma}\right]\right]. \tag{B6}$$

In the limit $\Gamma\to0$, Eq. (B5) becomes the result obtained by Safran,[28]

$$\chi = \frac{v^2e^2}{12\pi c^2 t}\left[f(-t)-f(t)+3\mathcal{P}\int_{-t}^{t}dx\frac{f(x)}{x}\right] \tag{B7}$$

$$=\frac{v^2e^2}{12\pi c^2 t}\theta(t-|\mu|)\left(1+3\log\left|\frac{\mu}{t}\right|\right)\quad(T=0), \tag{B8}$$

where $\mathcal{P}$ means the Cauchy's principal value. On the other hand, in the limit $t\to0$, we obtain a value two times of that of the monolayer system (19).

The derivation of the formula (18) for the 2×2 Hamiltonian (3) can be done in the same way as Ref. 40. In this calculation, we should extract terms of the thermodynamic potential which is proportional to squire of the magnetic field in the following representation:

$$B^2 = \frac{2q_+q_-A_+A_- - q_+^2A_-^2 - q_-^2A_+^2}{4}. \tag{B9}$$

The formula for $N=2$ was also derived in Ref. 30 using γ_x, γ_y which has more complicated expression. These two expressions can be shown to be equivalent using some identities. To calculate susceptibility for Eq. (3), a finite cutoff is needed to make the susceptibility finite. This result shows diamagnetism near the zero energy point, but it is not appropriate for quantitative analysis.

[1] K. S. Novoselov, A. K. Geim, S. V. Morozov, D. Jiang, M. I. Katsnelson, I. V. Grigorieva, S. V. Dubonos, and A. A. Firsov, Nature (London) **438**, 197 (2005).

[2] Y. Zhang, Y.-W. Tan, H. L. Stormer, and P. Kim, Nature (London) **438**, 201 (2005).

[3] A. W. W. Ludwig, M. P. A. Fisher, R. Shankar, and G. Grinstein, Phys. Rev. B **50**, 7526 (1994).

[4] N. H. Shon and T. Ando, J. Phys. Soc. Jpn. **67**, 2421 (1998).

[5] Y. Zheng and T. Ando, Phys. Rev. B **65**, 245420 (2002).

[6] V. P. Gusynin and S. G. Sharapov, Phys. Rev. Lett. **95**, 146801 (2005).

[7] V. P. Gusynin and S. G. Sharapov, Phys. Rev. B **73**, 245411 (2006).

[8] N. M. R. Peres, F. Guinea, and A. H. Castro Neto, Phys. Rev. B **73**, 125411 (2006).

[9] K. Ziegler, Phys. Rev. B **75**, 233407 (2007), and references therein.

[10] E. McCann and V. I. Fal'ko, Phys. Rev. Lett. **96**, 086805 (2006).

[11] J. Nilsson, A. H. Castro Neto, F. Guinea, and N. M. R. Peres, Phys. Rev. Lett. **97**, 266801 (2006).

[12] M. Koshino and T. Ando, Phys. Rev. B **73**, 245403 (2006).

[13] J. Cserti, Phys. Rev. B **75**, 033405 (2007).

[14] J. Cserti, A. Csordas, and G. David, Phys. Rev. Lett. **99**, 066802 (2007).

[15] T. Ohta, A. Bostwick, J. L. McChesney, T. Seyller, K. Horn, and E. Rotenberg, Phys. Rev. Lett. **98**, 206802 (2007).
[16] A. Bostwick, T. Ohta, J. L. McChesney, K. V. Emtsev, T. Seyller, K. Horn, and E. Rotenberg, arXiv:0705.3705 (unpublished).
[17] S. Y. Zhou, G.-H. Gweon, A. V. Fedorov, P. N. First, W. A. de Heer, D.-H. Lee, F. Guinea, A. H. Castro Neto, and A. Lanzara, Nat. Mater. **6**, 770 (2007).
[18] B. Partoens and F. M. Peeters, Phys. Rev. B **74**, 075404 (2006).
[19] S. Latil and L. Henrard, Phys. Rev. Lett. **97**, 036803 (2006).
[20] F. Guinea, A. H. Castro Neto, and N. M. R. Peres, Phys. Rev. B **73**, 245426 (2006).
[21] J. L. Mañes, F. Guinea, and María A. H. Vozmediano, Phys. Rev. B **75**, 155424 (2007).
[22] J. W. McClure, Phys. Rev. **104**, 666 (1956).
[23] S. A. Safran and F. J. DiSalvo, Phys. Rev. B **20**, 4889 (1979).
[24] A. Ghosal, P. Goswami, and S. Chakravarty, Phys. Rev. B **75**, 115123 (2007).
[25] H. Fukuyama, J. Phys. Soc. Jpn. **76**, 043711 (2007).
[26] M. Koshino and T. Ando, Phys. Rev. B **75**, 235333 (2007).
[27] M. Nakamura, Phys. Rev. B **76**, 113301 (2007).
[28] S. A. Safran, Phys. Rev. B **30**, 421 (1984).
[29] R. Saito and H. Kamimura, Phys. Rev. B **33**, 7218 (1986).
[30] M. Koshino and T. Ando, Phys. Rev. B **76**, 085425 (2007).
[31] For example, see G. D. Mahan, *Many-Particle Physics* (Plenum, New York, 2000).
[32] For example see A. A. Abrikosov, L. P. Gorkov, and I. E. Dzyaloshinski, *Methods of Quantum Field Theory in Statistical Physics* (Dover, New York, 1965).
[33] K. Nomura and A. H. MacDonald, Phys. Rev. Lett. **98**, 076602 (2007).
[34] N. M. R. Peres, J. M. B. Lopes dos Santos, and T. Stauber, Phys. Rev. B **76**, 073412 (2007).
[35] J. M. Luttinger and W. Kohn, Phys. Rev. **97**, 869 (1955).
[36] H. Fukuyama, H. Ebisawa, and Y. Wada, Prog. Theor. Phys. **42**, 494 (1969).
[37] H. Fukuyama, Ann. Phys. (Leipzig) **15**, 520 (2006).
[38] X. Yang and C. Nayak, Phys. Rev. B **65**, 064523 (2002).
[39] S. V. Morozov, K. S. Novoselov, F. Schedin, D. Jiang, A. A. Firsov, and A. K. Geim, Phys. Rev. B **72**, 201401(R) (2005).
[40] H. Fukuyama, Prog. Theor. Phys. **45**, 704 (1971).
[41] Y. Maeda, C. Hotta, and M. Oshikawa, Phys. Rev. Lett. **99**, 057205 (2007).
[42] For example, see M. Sato and M. Oshikawa, Phys. Rev. B **75**, 014404 (2007).